Proc. Natl. Acad. Sci. USA
Vol. 85, pp. 5449–5453, August 1988
Biochemistry

Evidence for the direct involvement of the rhinovirus canyon in receptor binding

(viral attachment site/infectious cDNA/site-directed mutagenesis)

RICHARD J. COLONNO*, JON H. CONDRA, SATOSHI MIZUTANI, PIA L. CALLAHAN, MARY-ELLEN DAVIES, AND MARK A. MURCKO

Department of Virus and Cell Biology, Merck Sharp and Dohme Research Laboratories, West Point, PA 19486

Communicated by Edward M. Scolnick, April 6, 1988

ABSTRACT **Evidence is presented that indicates a deep crevice located on the surface of human rhinovirus type 14 is involved in virion attachment to cellular receptors. By using mutagenesis of an infectious cDNA clone, 11 mutants were created by single amino acid substitutions or insertions at positions 103, 155, 220, 223, and 273 of the structural protein VP1. Seven of the recovered mutants had a small plaque phenotype and exhibited binding affinities significantly lower than wild-type virus. One mutant, in which glycine replaced proline at amino acid position 155, showed a greatly enhanced binding affinity. Single-cycle growth kinetics suggested that 5 of the mutants had delayed growth cycles due to intracellular deficiencies apart from receptor binding.**

Human rhinoviruses (HRVs) are members of the Picornaviridae and are the major causative agent of the common cold (1). Previous studies have indicated that HRV serotypes can be divided into "major" (78 serotypes) and "minor" (10 serotypes) groups (2, 3). Information regarding the identity and characterization of picornavirus receptors, in general, is quite limited and has been reviewed (4). Much of the information on picornavirus receptors has been obtained through the use of monoclonal antibodies directed toward cell surface components involved in viral attachment (4). The most useful of these antibodies has been one that specifically blocks attachment of the major group of HRVs (3). By using this anti-receptor antibody (designated antibody 1A6), a 90-kDa receptor glycoprotein was isolated from human and chimpanzee cells and shown to be directly involved in attachment by the major group of HRVs (5).

Little is known about the structure and location of the viral attachment site of HRVs that interacts with cellular receptors. Since this receptor is shared by at least 78 antigenically distinct serotypes, it was puzzling that the infected host could not elicit a cross-neutralizing response to such a highly conserved surface feature. Crystallographic studies on HRV type 14 (HRV-14), a major HRV group virus, and poliovirus have shed much light on this problem (6, 7). Among the many structural features determined for these two viruses was the discovery of a deep canyon present on the surface of the viral capsid. Based on RNA genome sequences, a similar canyon structure most likely exists within the capsid structures of type B coxsackieviruses (8). Rossmann *et al.* (6) initially proposed that this deep canyon structure might serve as the virion attachment site, since it is too narrow to allow access to an immunoglobulin. There is precedent for involvement of a surface crevice, since a surface depression found on the hemagglutinin protein of influenza virus has been shown to be involved in receptor binding (9).

The publication costs of this article were defrayed in part by page charge payment. This article must therefore be hereby marked "*advertisement*" in accordance with 18 U.S.C. §1734 solely to indicate this fact.

The present study provides strong evidence that the HRV canyon is indeed involved in attachment by constructing HRV-14 mutants that have altered amino acids within the virion canyon and demonstrating that the resultant mutant viruses have altered binding phenotypes.

MATERIALS AND METHODS

Structure of HRV-14. Refined coordinates of HRV-14 were kindly provided by Michael Rossmann and his colleagues at Purdue University (West Lafayette, IN). Coordinates were viewed by using the FRODO program with an Evans & Sutherland PS330 graphics terminal.

Mutagenesis. Oligonucleotide-directed mutants were constructed by a modification of the gapped-duplex mutagenesis method (10). Plasmid pSP64(RV) DNA (11) was cut with *Dra* III and digested with nuclease BAL-31 (slow form; International Biotechnologies, New Haven, CT) for 30 min, to delete 350–400 base pairs from each end. The DNA (0.1 μg) was mixed with 0.1 μg of *Sma* I-digested pSP64(RV) DNA and 40 pmol of the mutagenic oligonucleotide in 10 μl of a solution containing 0.2 M NaCl, 12 mM Tris·HCl (pH 7.5), 11 mM $MgCl_2$, and 2 mM 2-mercaptoethanol. Denaturation, annealing, and polymerization were as described (10), except that *Escherichia coli* DNA ligase and 50 μM NAD were substituted for T4 DNA ligase and ATP in the reaction mix. Plasmids were grown in *E. coli* AG-1 (StrataGene), and minipreps of mutant colonies were used to confirm the locations of mutations by Southern blotting (12) and as a source of DNA to retransform AG-1 cells for purification of mutant plasmids.

For insertion mutagenesis, plasmid pSP64(RV) was partially digested with *Dde* I and full-length linear DNA molecules were isolated by agarose gel electrophoresis (13). The 5′ overhangs were filled-in by using the Klenow fragment of DNA polymerase I and the DNA was religated (14). After transformation, plasmid DNAs were mapped by restriction endonuclease digestion.

Transfection of Infectious RNA. DNA was transcribed *in vitro* and 1 μg of RNA was used to transfect HeLa cells as described (11). Medium of transfected cells was changed every 3 days, and cells usually had extensive cytopathology in 2–7 days. Recovered virus was plaque purified before large-scale virus propagation. All recovered viruses were neutralized by anti-HRV-14 antiserum.

Virus, Cells, Antibody, and Membranes. Procedures used to propagate, purify, radiolabel, and titrate HRVs in HeLa R-19 cells have been described (2). Plaque diameters were determined by measuring 40 plaques on two separate occasions and averaging the diameters obtained. The isolation,

Abbreviations: HRV, human rhinovirus; HRV-14 and -15, HRV types 14 and 15, respectively; pfu, plaque-forming units; wt, wild type.

*To whom reprint requests should be addressed.

purification, and use of anti-receptor monoclonal antibody 1A6 have been described (3). Crude membrane preparations were isolated from HeLa cells and used in membrane binding assays as detailed elsewhere (3).

Single and Multiple-Cycle Growth Curves. Single-cycle growth kinetics were obtained by infecting confluent HeLa cell monolayers in 48-well cluster plates in duplicate at a multiplicity of 100 plaque-forming units (pfu) per cell in a volume of 0.1 ml. After 1.5 hr, the inoculum was removed; cells were washed five times with 250 μl of warm McCoy's 5A medium containing 2.5% (vol/vol) fetal calf serum, 20 mM Hepes (pH 7.4), and 10 mM $MgCl_2$; 0.1 ml of warm medium was then added to each well; and plates were incubated at 34°C. Plates were placed at −70°C at the times indicated, and each plate was frozen and thawed three times prior to the plaque assay (2). Multiple-cycle growth kinetics were performed in essentially the same manner, except for infection at a multiplicity of 0.5 pfu per cell and incubation for 58 hr.

Scatchard Analysis. The particle to cpm ratios of HRV preparations propagated in the presence of [^{35}S]methionine were determined by electron microscopy and scintillation counting, respectively. Increasingly higher concentrations of radiolabeled virus were added to HeLa cell monolayers (1–2.5 × 10^5 cells per well) for 1 hr at 34°C in the presence or absence of 4.5 μg of antibody 1A6. After incubation for 1 hr, medium was removed and each monolayer was washed with medium and then treated with 1% $NaDodSO_4$. The amount of radioactivity found in the bound and unbound fractions was determined, and specific binding was calculated by subtracting binding values obtained in the presence of antibody. The resulting data were used with the EBDA program (distributed by Elsevier-BIOSOFT, Cambridge, U.K.).

RESULTS

The Rhinovirus Canyon. Examination of HRV-14 at the atomic level has revealed many facets of the virion structure (6). Of particular interest was the observation that a deep canyon exists on the surface of the virus encircling each of the 12 vertices with fivefold symmetry that compose the icosahedral-shaped capsid. Due to the oscillating shape of the canyon, it is difficult to directly visualize the depth and contour of this structure. Fig. 1 is a schematic representation in which the foreground and background are removed to visualize the width and depth of the canyon. This particular portion of the canyon is 35 Å wide at the opening and narrows to only 16 Å near the bottom. The deepest regions of the canyon are 22 Å from the surface.

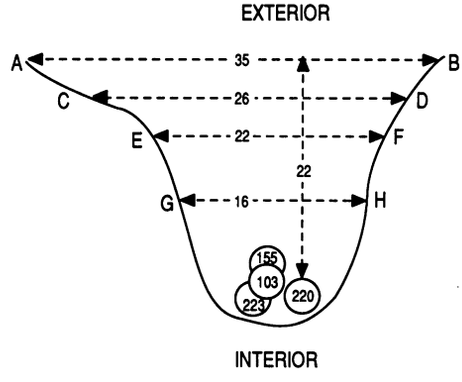

FIG. 1. Schematic representation of the HRV-14 canyon. Distances are shown in angstroms and circled numbers represent the four amino acids targeted in these studies. Coordinate points in VP1 used in determining distances are as follows: A, $O^{\delta 1}$ of Asp-91; B, $O^{\epsilon 2}$ of Glu-210; C, $O^{\delta 1}$ of Asn-92; D, O Glu-210; E, $O^{\epsilon 2}$ of Glu-95; F, $N^{\epsilon 2}$ of Gln-212; G, $O^{\delta 2}$ of Asp-101; and H, $C^{\delta 1}$ of Ile-215.

Close examination of the canyon floor and walls focused our attention on four amino acids residing within a radius of 5 Å. These four amino acids, Lys-103, Pro-155, Ser-220, and His-223, are located in the VP1 and highlighted in the stereo diagram in Fig. 2. These amino acids were of interest because they reside in the deepest region of the canyon and have side chains that protrude upward from the floor of the canyon.

Mutagenesis of an Infectious cDNA Clone. To determine if these four amino acids influenced the ability of the virus to bind to cellular receptors, 10 mutants were constructed by oligonucleotide-directed mutagenesis of an infectious HRV-14 cDNA (11). The selected amino acid changes represented both conservative and radical substitutions within VP1 (Table 1), so as to possibly pick up variable effects at each site. A second approach, utilizing random-insertion mutagenesis, yielded only one mutant mapping to an exposed region of the canyon. This mutant inserted an asparagine after amino acid 273 of VP1.

The modified cDNAs were transcribed into infectious RNA and used to transfect HeLa cells. Progeny virus was recovered and plaque purified, and working stocks were prepared. To eliminate the possibility of additional mutations or reversions during viral growth and passage, genome RNA was isolated from progeny virus and the regions encoding the capsid proteins were resequenced. Only the Tyr-155 construction failed to generate progeny virus after repeated attempts. Since the sequence of this mutant was correct, we can only assume that this modification is lethal for undefined reasons.

Growth Characteristics of Viral Mutants. Plaque titrations demonstrated that 8 of the 10 viable mutants had altered plaque morphologies (Table 1). Only the Asn-103 and Asn-273 mutants had plaque diameters near that of wt HRV-14. Since HRVs characteristically produce heterogenously sized plaques, more quantitative data were obtained by determining the progeny yields 58 hr after low-multiplicity infections. Results (Table 1) confirmed the plaque data and showed a direct correlation between small plaque diameter and reduced virus yields after 58 hr. These results made it apparent that some of the amino acid substitutions had drastically altered the normal infectious cycle of the resultant virus. The Pro-155 and His-220 positions, in particular, were most sensitive to changes, as witnessed by a >90% drop in virus production after 58 hr.

Altered Binding Phenotypes. Membrane binding assays were used to directly compare the binding of each of the mutants to wt HRV-14. The results (Fig. 3) showed that the mutants could be divided into three groups. The first group, containing 7 of the 10 viable mutants, showed reduced binding capabilities that ranged from 50% to 10% of wt control values. In fact, the binding of the Trp- and Ile-220 mutants was barely detectable above background. The second group was composed of the Arg- and Ile-103 mutants and demonstrated binding capabilities approximately equivalent to that displayed by wt HRV-14. The surprising mutant, and sole member of the third group, was the Gly-155 mutant that demonstrated enhanced binding capabilities that were superior to wt HRV-14 in regard to binding kinetics and total virus bound.

Single-Cycle Growth Kinetics. Binding phenotypes did not correlate very well with the plaque size of the respective mutant viruses. This was particularly evident for the Gly-155 mutant, which had an enhanced binding affinity and reduced plaque diameter. These results suggested that the amino acid substitutions were affecting additional viral processes distinct from attachment. To demonstrate this point, HeLa cells were infected at a high multiplicity of infection to compensate for differences in binding affinity and the production of infectious virions was measured hourly. The single-cycle growth curves in Fig. 4 show that Asn-, Ile-, and Arg-103, in addition to the Asn-273 and the Thr-223 mutants, had single-cycle growth curves equivalent to wt virus and that the multicycle growth

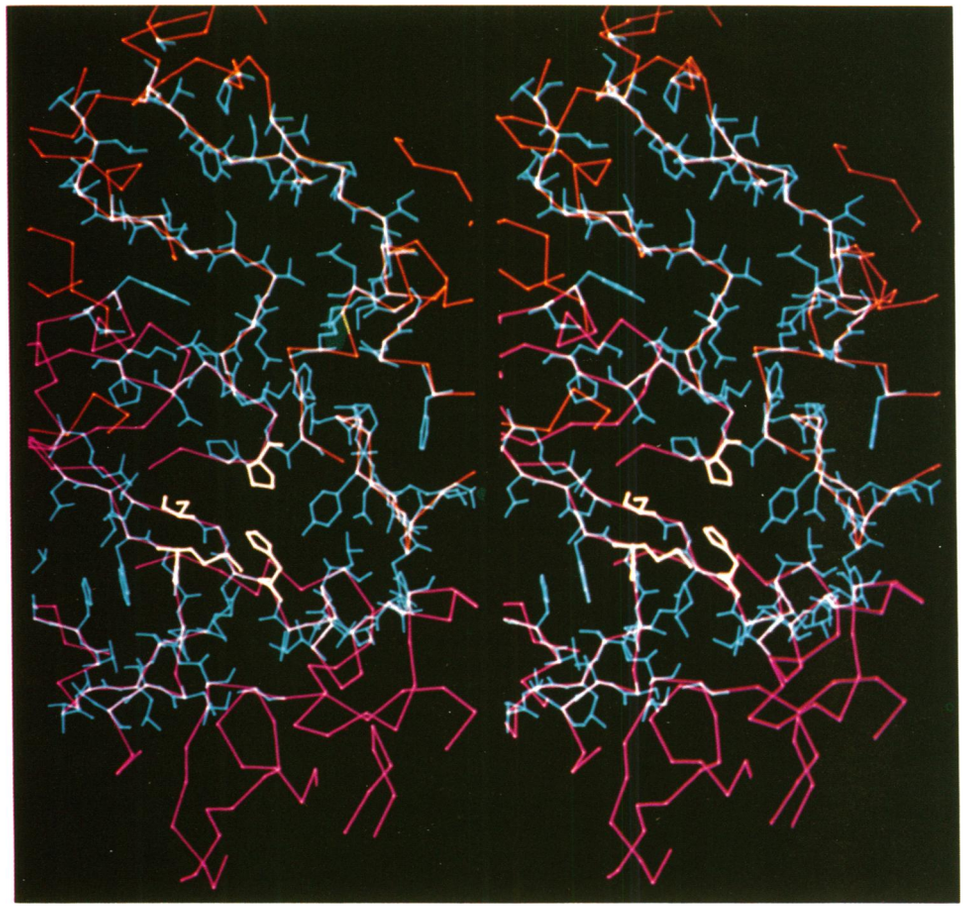

FIG. 2. Stereo diagram of canyon floor. The diagram uses a stereo representation to view the special arrangement of C^{α} atoms located in the vicinity of the bottom of the canyon. Residues belonging to VP1 and VP3 are shown in red and orange, respectively. The structures of the four amino acids selected for site-directed mutagenesis, Lys-103, Pro-155, His-220, and Ser-223, are highlighted in white, and the side chains of other residues exposed in the canyon are shown in blue. The view is looking down into the canyon from the outside of the virus.

curves (Table 1) obtained for these viruses are reflective solely on their inability to attach to cells normally. The Asn- and Ala-223 mutants, and more so with the Trp- and Ile-220 mutants, demonstrated delayed infectious cycles that strongly suggest that intracellular events may also be affected. The Gly-155 mutant was again most interesting since it repeatedly showed equivalent kinetics up to 10 hr after infection before the production of virus was delayed.

Virion Displacement. Virion displacement studies were performed to directly compare the binding affinities of wt HRV-14, HRV type 15 (HRV-15), and the Gly-155 and Ala-223 mutants. Earlier studies indicated that antibody 1A6 was capable of releasing bound virus from virus-membrane complexes (3). In an extension of these studies, we attempted to displace bound virions with other viruses. Representative data from such an experiment (Table 2) show that wt HRV-14 binds less strongly to receptors than HRV-15, since the latter can displace 38% of the bound HRV-14 virions. The molecule with the strongest affinity for the receptor is antibody 1A6, which can easily displace serotypes belonging to the major HRV group. Analysis of the two mutant viruses confirmed that the Gly-155 mutant has a binding affinity superior to wt HRV-14 and equal to or greater than HRV-15. In fact, even antibody 1A6 was only able to displace 51% of bound Gly-155 virions compared to 90% and 72% for HRV-14 and HRV-15, respectively. In contrast, >40% of the Ala-223 mutant was displaced by the weakly binding wt HRV-14 and virtually all of this mutant virus was displaced by HRV-15 and antibody 1A6.

Table 1. Growth characteristics of mutant viruses

Virus	Plaque diameter, mm	Virus yield,* pfu per cell
wt	3.7	160
Lys-103 → Ile	2.6	84
Arg	2.8	54
Asn	3.3	140
Pro-155 → Gly	1.0	14
Tyr	ND	ND
His-220 → Ile	0.8	10
Trp	0.9	14
Ser-223 → Ala	1.2	8
Thr	2.8	70
Asn	2.3	88
Asn-273 (I 273)	3.4	108

wt, Wild-type HRV-14; ND, not determined due to failure to recover viable virus.
*Determined by plaque assay 58 hr after infection.

Scatchard Analysis. To determine the precise binding affinity of the Gly-155 mutant compared to wt HRV-14 and HRV-15, saturation binding studies were generated with purified ^{35}S-labeled viruses (data not shown). All three viruses exhibited receptor saturation and specific binding, since parallel assays in the presence of excess antibody 1A6 showed negligible binding. Data points representing specific binding were used to obtain Scatchard plots (Fig. 5). It became obvious from the slopes obtained that the three viruses had different dissociation constants. The calculated K_d values for wt HRV-14, HRV-15, and the Gly-155 mutant virus were 4.35×10^{-11} M, 1.47×10^{-11} M, and 4.74×10^{-12} M, respectively, and indicate that the Gly-155 mutant has a K_d higher by a factor of 9 than HRV-14 and higher by a factor of 3 than HRV-15. Based on the B_{max} obtained for each virus, there are 1000–2000 virus receptors on each HeLa R-19 cell.

DISCUSSION

Although several viral attachment proteins have been identified, such as the type S adenovirus fiber protein (15), the σ1

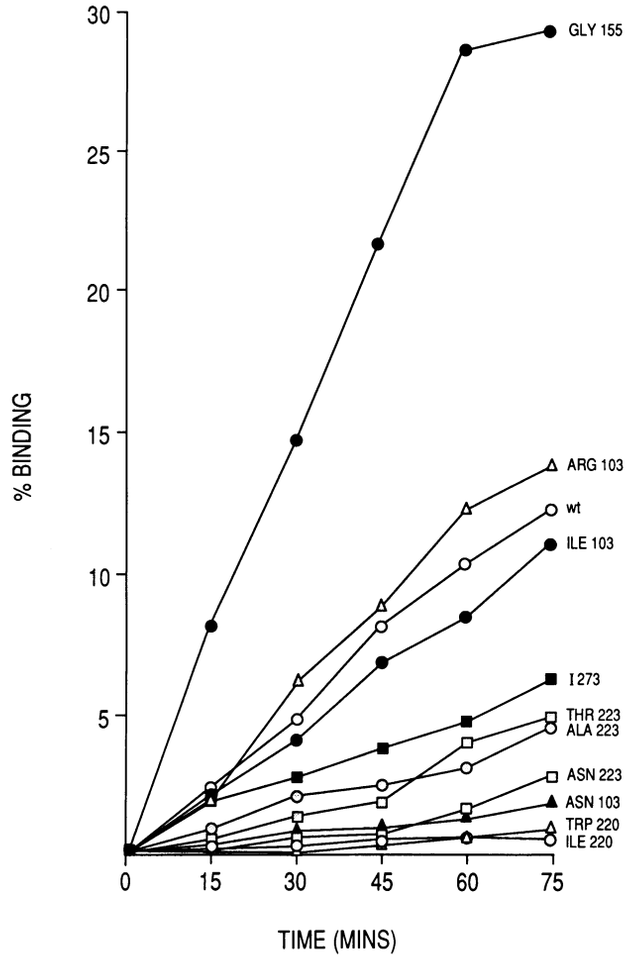

FIG. 3. Binding kinetics of HRV-14 mutants. Gradient-purified viruses, labeled with [^{35}S]methionine and representing each of the 10 mutant viruses and wt virus, were used in membrane binding assays. After incubation at 25°C for the times indicated, membranes were pelleted and the percent of virus specifically associated with the cell pellet was determined. All data points represent specific binding, since binding values obtained in the presence of antibody 1A6 have been subtracted.

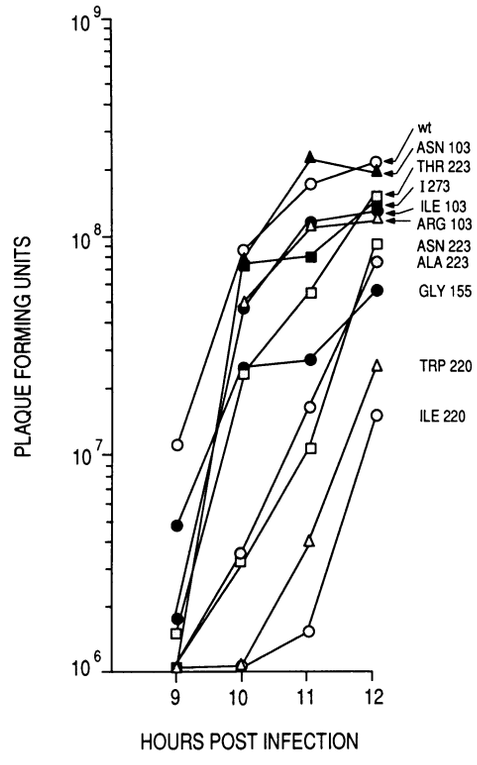

FIG. 4. Single-cycle growth curves of wt and mutant HRVs. Confluent HeLa cell monolayers were infected at a multiplicity of infection of 100 pfu per cell. After 1 hr at 34°C, the viral inoculum was removed, and cells were washed and incubated at 34°C. At each time point indicated, a 48-well cluster plate, containing cells infected with each of the viruses tested, was frozen and thawed twice, and the titer of infectious virus was determined by plaque assay.

protein of reovirus (16), and the hemagglutinin protein of influenza virus (17), no picornavirus proteins have been identified as attachment proteins. This is not surprising, since even mild disruption of the viral capsid seems to destroy the ability of the virus to bind to its receptor (unpublished data). This result strongly suggests that the virion attachment site may involve multiple proteins in a complex quaternary structure. Crystallographic studies on HRV-14 and poliovirus (6, 7) have enabled us to investigate the location of the virion attachment site at the atomic level. Rossmann *et al.* (6) suggested that a deep canyon found on the surface of the virus may be involved in receptor interaction.

The current studies use a direct approach to determine if the HRV-14 canyon is involved in receptor interaction. By using a HRV-14 infectious cDNA clone, a series of single amino acid changes was introduced into a region of VP1 that maps to a deep region of the canyon. A review of the data in Table 1, Table 2, and Fig. 3 suggests that the four amino acids at the floor of the canyon may be involved in receptor interaction. Replacing the positively charged lysine at position 103 with positively charged arginine or with a nonpolar isoleucine had no significant effect on virus binding. However, if a neutral polar asparagine residue was inserted at position 103, then the binding of the mutant was impaired. The changes at position 155 were interesting. Replacing Pro-155 with the smaller glycine resulted in a 9-fold increase in binding affinity, whereas a change to the larger tyrosine apparently is lethal. Amino acid position 220 was also very sensitive to substitution. Substituting the weakly charged histidine at position 220 with a nonpolar isoleucine or tryptophan generated mutant viruses with drastically reduced binding affinities. Similarly, replacement of the hydroxyl-containing serine at position 223 with an alanine or threonine resulted in mutants with decreased binding affinities. It is clear that the proper blend of size, charge, and hydrogen bonding properties in this region is critical for receptor protein interaction. Conversely, the insertion of an asparagine residue after

Table 2. Virion displacement studies

Challenge	% release of prebound virus			
	HRV-14	HRV-15	Gly-155 mutant	Ala-223 mutant
HRV-14	11	0	0	42
HRV-15	38	4	0	83
HRV-14 (Gly-155)	31	8	0	36
HRV-14 (Ala-223)	5	0	0	20
Antibody 1A6	90	72	51	99

Samples of ^{35}S-labeled virus were incubated with HeLa cell membranes for 1 hr at 25°C and virus–membrane complexes were pelleted by centrifugation as described (3). Pellets were washed with McCoy's 5A medium containing 1% fetal calf serum, 20 mM Hepes (pH 7.2), and 10 mM $MgCl_2$, repelleted, and resuspended in medium to their original volume. Medium or saturating amounts (10^8 pfu) of the unlabeled viruses indicated were added to bring each reaction mixture to 0.1 ml and the mixture was incubated at 25°C for 1 hr. Virus–membrane complexes were then pelleted, and the percent of radioactivity present in the membrane and supernatant fractions was determined.

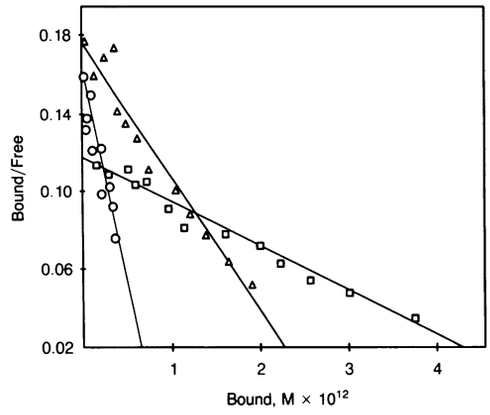

FIG. 5. Scatchard analysis of HRV binding data. Data obtained from the saturation binding curves of wt HRV-14 (□), HRV-15 (△), and the Gly-155 mutant (○) were used to develop Scatchard plots of the binding of each virus.

amino acid 273 resulted in progeny virus having near-normal binding and growth characteristics. This result would suggest that the region around residue 273, which is distal from the canyon floor and 25–30 Å from the location of the other four amino acids, is not directly involved with receptor interaction.

Single-cycle growth kinetics (Fig. 4) showed that five of the mutant viruses had significantly slower growth curves than wt HRV-14. Since all of these mutations are restricted to the structural protein VP1, enzymes, such as the viral-encoded protease and replicase, should not be directly affected. It is more likely that the newly introduced amino acid changes somehow alter the configuration of the P1 precursor protein such that proper proteolytic cleavage or maturation is impaired. This may be the reason why there is not a natural selection for glycine at position 155 in HRV serotypes. Four other mutants, Asn- and Ala-223 and Trp- and Ile-220, also had retarded single-cycle growth curves suggestive of replicative problems apart from their receptor binding deficiencies.

The ability to displace bound virions from receptors was used to compare the binding affinities of the Gly-155 and Ala-223 mutants with wt HRV-14 and HRV-15. The Gly-155 mutant demonstrated the strongest affinity, whereas the Ala-223 mutant was easily displaced by wt HRV-14. More direct measurement of receptor affinities was obtained by Scatchard analysis. The K_d values obtained clearly show the enhanced binding affinity of the Gly-155 mutant. With a K_d equal to 4.74^{-12} M, the binding of the Gly-155 mutant is greater than wt HRV-14 by a factor >9. Attempts to determine the K_d of the weaker binding mutants, such as the Ala-223 mutant, were unsuccessful due to the inability to obtain sufficient saturation binding curves for Scatchard plots.

The altered binding phenotypes displayed by these mutants represent strong evidence that the canyon floor is somehow involved in receptor interaction. It is not known whether the observed binding affinities were the result of simple charge changes or reflect gross anatomical changes in neighboring amino acids on the floor of the canyon. However, the possibility is remote that these changes could have affected structures outside of the canyon since a rippling effect, involving numerous amino acids, would be needed to significantly alter external structures some 22 Å away. The region selected for amino acid substitutions is one that is highly conserved, not only among HRV serotypes, but also in a number of other picornaviruses. It is highly unlikely that this particular region is involved in determining receptor specificity. Instead, it is more probable that this conserved region may interact with a common domain found on several receptors and that it is the shape and contour of the canyon entrance that define the accessibility of a receptor protein into the viral canyon. Further studies will help to determine if other regions of the canyon are involved in receptor interaction.

1. Hamparian, V. V., Colonno, R. J., Cooney, M. K., Dick, E. C., Gwaltney, Jr., J. M., Hughes, J. H., Jordan, Jr., W. S., Kapikian, A. Z., Mogabgab, W. J., Monto, A., Phillips, C. A., Rueckert, R. R., Schieble, J. H., Stott, E. J. & Tyrrell, D. A. J. (1987) *Virology* **159,** 191–192.
2. Abraham, G. & Colonno, R. J. (1984) *J. Virol.* **51,** 340–345.
3. Colonno, R. J., Callahan, P. L. & Long, W. J. (1986) *J. Virol.* **57,** 7–12.
4. Colonno, R. J. (1987) *BioEssays* **5,** 270–274.
5. Tomassini, J. E. & Colonno, R. J. (1986) *J. Virol.* **58,** 290–295.
6. Rossmann, M. G., Arnold, E., Erickson, J. W., Frankenberger, E. A., Griffith, J. P., Hecht, H.-J., Johnson, J. E., Kamer, G., Luo, M., Mosser, A. G., Rueckert, R. R., Sherry, B. & Vriend, G. (1985) *Nature (London)* **317,** 145–153.
7. Hogle, J. M., Chow, M. & Filman, D. J. (1985) *Science* **229,** 1358–1365.
8. Jenkins, O., Booth, J. D., Minor, P. D. & Almond, J. W. (1987) *J. Gen. Virol.* **68,** 1835–1848.
9. Rogers, G. N., Paulson, J. C., Daniels, R. S., Skehel, J. J., Wilson, I. A. & Wiley, D. C. (1983) *Nature (London)* **304,** 76–78.
10. Morinaga, Y., Franceschini, T., Inouye, S. & Inouye, M. (1985) *BioTechnology* **2,** 636–639.
11. Mizutani, S. & Colonno, R. J. (1985) *J. Virol.* **56,** 628–632.
12. Southern, E. (1975) *J. Mol. Biol.* **98,** 503–517.
13. Wieslander, L. (1979) *Anal. Biochem.* **98,** 305–309.
14. Bernstein, H. D., Sonenberg, N. & Baltimore, D. (1985) *Mol. Cell. Biol.* **5,** 2913–2923.
15. Dorsett, P. H. & Ginsberg, H. S. (1975) *J. Virol.* **15,** 208–216.
16. Lee, P. W. K., Hayes, E. C. & Joklik, W. K. (1981) *Virology* **108,** 156–163.
17. Paulson, J. C. (1985) in *The Receptors,* ed. Conn, P. M. (Academic, London), Vol. 2, pp. 131–219.